**High Burn-up Spent Nuclear Fuel Structural Response When Subjected to a Hypothetical Impact AccidentProceedings of PVP 2004:
Pressure Vessels and Piping Conference
La Jolla, San Diego, California
July 25-29, 2004**

Spent Nuclear Fuel Structural Response When Subject to an End Impact AccidenT

David T. Tang, Jack Guttmann
United States Nuclear Regulatory Commission, Rockville, MD, USA

, Washington, DC, USA; Brian J. Koeppel, Richland, WA, USA; Harold E. Adkins
Pacific Northwest National Laboratory, Richland, WA, USA
, Richland, WA, USA

1. Abstract

The US Nuclear Regulatory Commission (USNRC) is responsible for licensing spent fuel storage and transportation systems. A subset of this responsibility is to investigate and understand the structural performance of these systems. Studies have shown that the fuel rods of intact spent fuel assemblies with burn-ups up to 45 gigawatt days per metric ton of uranium (Gwd/MTU) are capable of resisting the normally expected impact loads subjected during drop accident conditions. However, effective cladding thickness for intact spent fuel assemblies with burn ups greater than 45 Gwd/MTU can be reduced due to corrosion. The capability of the fuel rod to withstand the expected loads encountered under normal and accident conditions may also be reduced, given degradation of the material properties under extended use, such as decrease in ductility. The USNRC and Pacific Northwest Laboratory (PNNL) performed computational studies to predict the structural response of spent nuclear fuel in a transport system that is subjected to a hypothetical regulatory impact accident, as defined in 10 CFR71.73.[1] This study performs a structural analysis of a typical high burn up pPressurized Wwater Rreactor (PWR) fuel assembly using the ANSYS®ANSYS®/LS- DYNA®TM [2] finite element analysis (FEA) code. The material properties used in the analyses were based on expert judgment and included uncertainties. Ongoing experimental programs will reduce the uncertainties. The current evaluations include the pins, spacer grids, and tie plates to assess possible cladding failure/rupture under hypothetical impact accident loading. This paper describes the USNRC and PNNL staff's analytical approach, provides details on the single pin model developed for this assessment, and presents the results.

2. Introduction

A renewed interest in examining more closely the structural integrity of fuel pins under storage handling and hypothetical transportation accident conditions has arisen from a recent initiative to store and transport high burn-up (45 to 75 GWd/MTU) fuels. Cladding failure may assume a variety of modes depending on loading conditions, fuel geometry, and material properties. It was found in the report SAND90-2406[3],[2], in general, that the pressurized water reactor (PWR) fuel cladding was more vulnerable to impact events than the boiling water reactor (BWR) cladding. For the axial loading and inelastic buckling of a representative PWR fuel pin at a prescribed 100-G acceleration, the report computed maximum bending strains of approximately 2% with lateral restraint and 8% at incipient collapse without lateral restraint.

Experimental tests are being conducted to generate mechanical property and toughness data for high burn-up fuel cladding materials. Based on information to date, total elongation (ductility) of high burn-up fuel cladding is anticipated to range from 1.0% to 2.8%. This is the same order of magnitude as that previously calculated by Sandia National Laboratories[2].[3]

3. Modeling Approach

The main objective of this study was to use a numerical model to compute the inelastic buckling capacity and corresponding strain ductility demands for a representative spent fuel assembly pin under a simulated cask handling or drop accident as defined in Code of Federal Regulations, Title 10, Part 71, Subpart 73

(10 CFR71.73)[3]. This will be approached by modeling at several levels. Because the impact event entails the interaction of hundreds of pins, their spacer grids, tie plates, fuel spacers, basket, cask, and impact limiters under dynamic loading, this simulation can be computationally expensive. For computational efficiency it is desirable to model a single pin as was done in some previous studies[2,6] [3,4] to provide a simpler method to evaluate the buckling behavior of a fuel pin. This model contains several assumptions to provide a conservative analysis. A more detailed analysis to evaluate the response of an entire assembly due to a detailed cask response is the next step and in progress. This will provide a more realisticcomprehensive assessment of the assembly dynamic response and verification of the single pin assumption. To assess failure rates for the pin cladding, should it be required, probabilistic fracture analyses will be pursued based on the stress results. This paper describes the explicit dynamic analysis of the finite element analysis (FEA) model developed for evaluating the single pin subjected to end impact loads and parametric analysis results. More detailed description of the modeling approach is also provided in [85].

There are a number of conservative assumptions in the single pin pin approximation. This approach assumes that all pins in an assembly experience the same deformation due to an impact event. The single pin response is then characteristic of all pins and can be studied independently. The other components of the transport system are also modeled in minimal detail for computational efficiency. The cask is modeled as a point mass to capture pin-cask dynamics, the impact limiter is modeled as a constant force-deflection spring, and the spacer grids are modeled as nonlinear springs to provide lateral support to the pin with a prescribed force-deflection curve. For conservatism, it was desired to eliminate the contribution of the fuel pellet to the pin bending stiffness. This assumption, which is consistent with typical fuel pin buckling analyses, was selected to yield a conservative reference point by discounting the contribution of the fuel pellets to the pin's flexural rigidity but still considering 100% of their mass contribution. However, to overcome unrealistic ovalization of the open cross section on lateral deformation, nonlinear single degree-of-freedom springs were included to represent a Hertzian-type radial contact between the cladding and the fuel during lateral loading.

ANSYS® was used in this study for general model development, whereas the explicit solution was performed by the LS-DYNA®TM solver implemented in the ANSYS framework. Some of the model parameters that were varied include the impact deceleration, assembly-to-compartment gap, internal pin pressure, fuel effects, and pin geometry. The baseline fuel pin used in the study was a Babcock & Wilcox (B&W) 15x15 pin geometry.

4. Model Description

The typical fuel assembly pin is composed of cylindrical fuel pellets within a tubular cladding material that has reinforced end thimbles and an internal spring to minimize the gap between the fuel pellets at all times. The pin was modeled using shell elements with appropriate thickness and diameter to represent the cladding. A drawing of the model representation for the single pin model is shown in Figure 1. It is composed of a single fuel pin, a lumped cask mass, springs representing the spacer grids, contact surfaces representing the compartment wall, and a spring representing the impact limiter. Several views of the actual finite element mesh are shown in Figure 2.

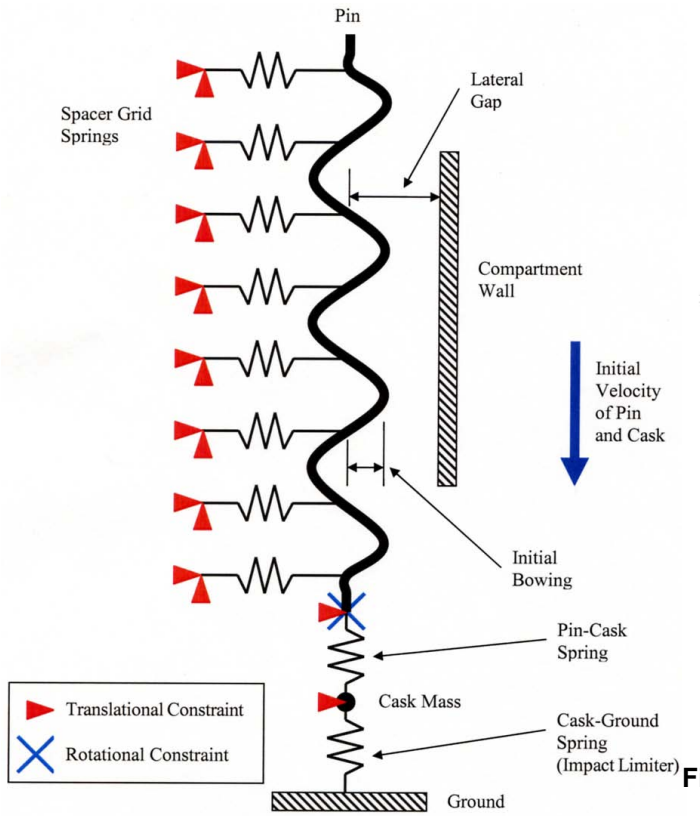

Figure 1. Pin geometry and boundary conditions.

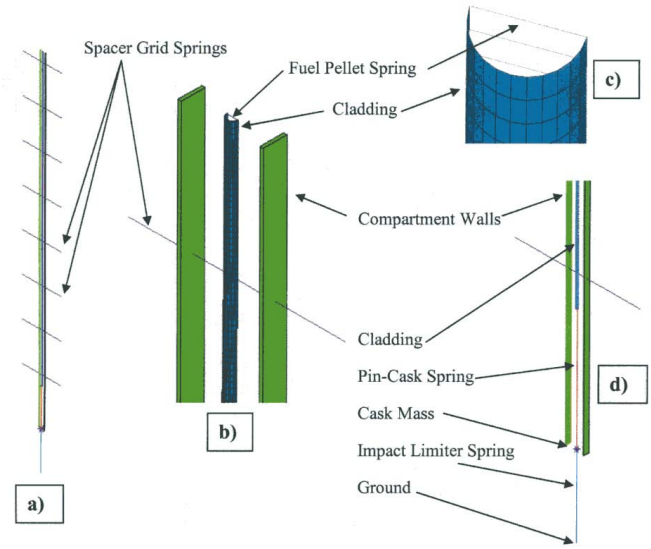

Figure 2. Pin finite element model.

4.1. Geometry

Fuel Pin: The pin was modeled with an initial bowed geometry between the spacer grids.[23] At the pin ends, it was assumed that they had no initial rotation and that this condition would exist due to the constraint provided by the upper and lower tie plates.

Spacer Grids: The spacer grids are arrayed structures that provide intermediate support to the fuel pins in the assembly. The grids are composed of small leaf springs that ensure proper spacing of the pins in the assembly array. The grids were assumed to provide lateral support to the pin at eight intermediate locations (Figure 1Figure 2Figure 2) according to the fuel geometry considered. This contribution was represented by sets of compression-only springs attached to each side of the cladding cross section.

Fuel Compartment: Deflection of the fuel pins during an impact event will lead to pin-to-pin and pin-to-compartment wall contact. During an impact event in which the pin buckles, the pins deform laterally until all pins are compressed against the compartment wall. To implement this behavior in a single-pin model, the total lateral distance over which a pin could deform was be determined. The gap was determined by considering the pin diameter, number of pins, and compartment width to determine the total free space in which the center pins in an assembly could unilaterally deform. The compartment walls were then modeled as rigid contact surfaces fixed in space at the proper lateral gap (Figure 2).

Pin-Cask-Impact Limiter Interaction: To include the effects of cask mass on system dynamics, the cask was modeled as a point mass connected by a compression-only spring to the pin bottom. A second compression-only spring was then used to simulate the impact limiter and contact with the rigid ground contact. This permitted the model to capture the impact of the target surface and any loss of contact between the pin and cask or the cask and ground.

4.2. Materials

Cladding: The temperature-dependent material properties for the Zircaloy cladding material were obtained from PNNL research on a companion project to estimate mechanical properties of high burn-up fuels. A uniform temperature of 500°F (260°C) was assumed for the pin, giving material property estimates of 10.981eE6 psi (75.7

GPa) for the elastic modulus, 92.4eE3 psi (637.1 MPa) for the yield strength, 94.4eE3 psi (650.9 MPa) for the tensile strength, and 0.404 for Poisson's ratio.

Fuel Pellet Spring: To simulate the fuel-clad interaction and its ability to limit gross cladding ovalization, the fuel pellet was modeled as an equivalent spring. The force-deflection curve for this spring was adapted from the solution of an elastic cylinder under Hertzian contact between two plates as defined by Roark.[76]

Spacer Grid Spring: The force-deflection curves for the spacer grid springs were adapted from Sanders.[23] The curves represent elastic deformations from a number of compounding events during the lateral compression of a fuel assembly, including 1) compression of the spacer grid leaf spring, 2) compression of the spacer grid frame, 3) buckling of consecutive spacer grid cells, and 4) crushing of the fuel pin cross section. The spacer grids at the top and bottom of the assembly are attached to the end plates and are consequently stiffer, so they are represented by a separate curve.

Cask-Ground Spring: The cask-ground spring represents the behavior of the impact limiter and is the major source of energy absorption in the system. The impact limiter is characterized by constant force deflection, where the force magnitude is defined by the product of the impact limiter area and the material crush strength. The spring is compression-only to permit the cask to lose contact with the ground when it rebounds. The assumed properties for a 128 in (325 cm) diameter impact limiter is 400eE3 psi (2.76 GPa) for the elastic modulus and 1050 psi (7.24 MPa) ffor the crush strength.

4.3. Boundary Conditions

In-plane rotation and lateral translation was constrained at the bottom of the pin based on the assumption that the pins will likely be "jammed" into the bottom tie plate and restrict rotation and lateral translation. Appropriate boundary conditions for the symmetry plane, spring, and ground nodes were also applied.

4.4. Loads

After a fuel assembly has been exposed to a neutron flux and burned for high burn-up durations (>45 GWd/MTU), internal pin pressures due to fission gas generation can range from 1000 to 2200 psi (6.89 to 15.16 MPa). A pressure loading of 1400 psi (9.65 MPa) was applied to the inner cladding surface, prior to the impact event, to simulate the effects of this fission gas generation. An initial velocity of 528 in/sec (1341 cm/s) (corresponding to the standard regulatory 30 ft (9 m.1) drop – 10 CFR71.73[3]) was applied to the pin and cask nodes.

5. Results and Discussion

The results for the remaining parametric cases in the sensitivity analyses are summarized in Table 1 followed by brief discussions of each case. In this table the "System Average Deceleration" represents the rigid body deceleration of the center of mass for the entire package (cask and all contents), the "Cask Maximum Deceleration" represents the rigid body deceleration of the center of mass for the cask, and the "Pin Maximum Deceleration" represents the rigid body deceleration of the center of mass for the fuel pin.

Table 1: Parametric Pin Buckling Analysis Results

Case #	System Average Deceleration (G)	Cask Maximum Deceleration (G)	Pin Maximum Deceleration (G)	Peak Tensile Strain (%)	Peak Compressive Strain (%)	Comments
1	**49**	**60**	**135**	**1.5**	**2.8**	**Baseline**
2	49	60	100	0.8	1.2	
3	41	50	118	1.2	2.2	
4	57	70	163	1.9	4.8	
5	49	60	148	1.1	2.2	
6	49	60	124	1.6	3.5	
7	49	60	120	2.0	5.5	
8	49	60	116	2.3	6.3	
9	42	50	111	1.9	3.6	
10	50	60	129	2.4	5.6	
11	59	70	138	2.7	6.5	
12	49	60	104	0.07	0.09	No Buckling

13	49	60	151	1.5	3.3	
14	49	60	126	1.3	2.6	

5.1. Baseline Case

The baseline case is performed with the B&W 15x15 fuel assembly pin geometry and is considered representative of typical transport cask systems in use. [23]. Presented in Figure 3 is a series of exaggerated deformed shapes of the assembly pin as the impact event progresses from initiation to rebound. Deformed shapes are presented for time starting at 0 ms (initiation) and plotted at intervals of 5 ms from left to right. The moving pin and cask nodes strike the ground and begin to decelerate. As the impact event progresses, the pin initiates buckling and begins to deflect laterally. Where the pin is held by the stiff spacer grid springs, the pin deflects very little and remains near the center of the enclosure. Large lateral deflections occur in the unsupported regions though, and the deflection direction alternates for each region (creating the expected sinusoidal-like deformation). This zonal lateral deflection continues until the pin reaches the contact surfaces representing its surrounding fuel pins fully deflected and against the fuel compartment wall. As the event progresses further, the long unsupported pin sections between spacer grids begin to flatten against the compartment wall, while the pin sections supported by the spacer grids remain at the center of the enclosure. As the flattened sections grow in length, the bending moment applied to the pin grows in the vicinity of the maximum curvature locations where the pin starts to contact the compartment wall. As the event continues and nears completion, the pin unloads and begins to rebound.

The rigid body acceleration history of the pin and cask is shown in Figure 4. It is observed that from 0-2 ms, the cask is decelerating due toas it contacts the ground. contact but At the same time, the pin must traverse the initial gap between the cask and its bottom. From 2-8 ms, the pin and cask are in contact with instantaneous pin decelerations of up to 110 G's. From 8-14 ms, the buckling instability occurs in the pin. From 14-28 ms, the pin and cask are again in contact until the system momentum is reduced to zero. Maximum instantaneous decelerations reach 135 G's for the pin. After 28 ms, the pin and cask rebound from the ground surface. Presented in Figure 5 is the global peak axial strain history for the pin, which is generated from the maximum instantaneous tensile and compressive axial strains anywhere in the cladding (i.e., the results are not from a single location). Despite the high magnitude of the peak pin deceleration (135 G's) (Figure 4), the peak tensile and compressive strains only reach magnitudes of 0.015 in/in and 0.028 in/in (or 1.5% and 2.8%), respectively. Presented in Figure 6 and Figure 7 are the instantaneous total axial strains and stresses, respectively, for t = 24.5 ms. As discussed earlier, as the flattened sections grow in length, the bending moment applied to the pin grows in the vicinity of the locations where the pin breaks contact with the compartment wall. These locations yield the highest stresses and strains, which are shown to be very localized. It should be noted again that the pin displacements in these figures have been exaggerated to display their behavior.

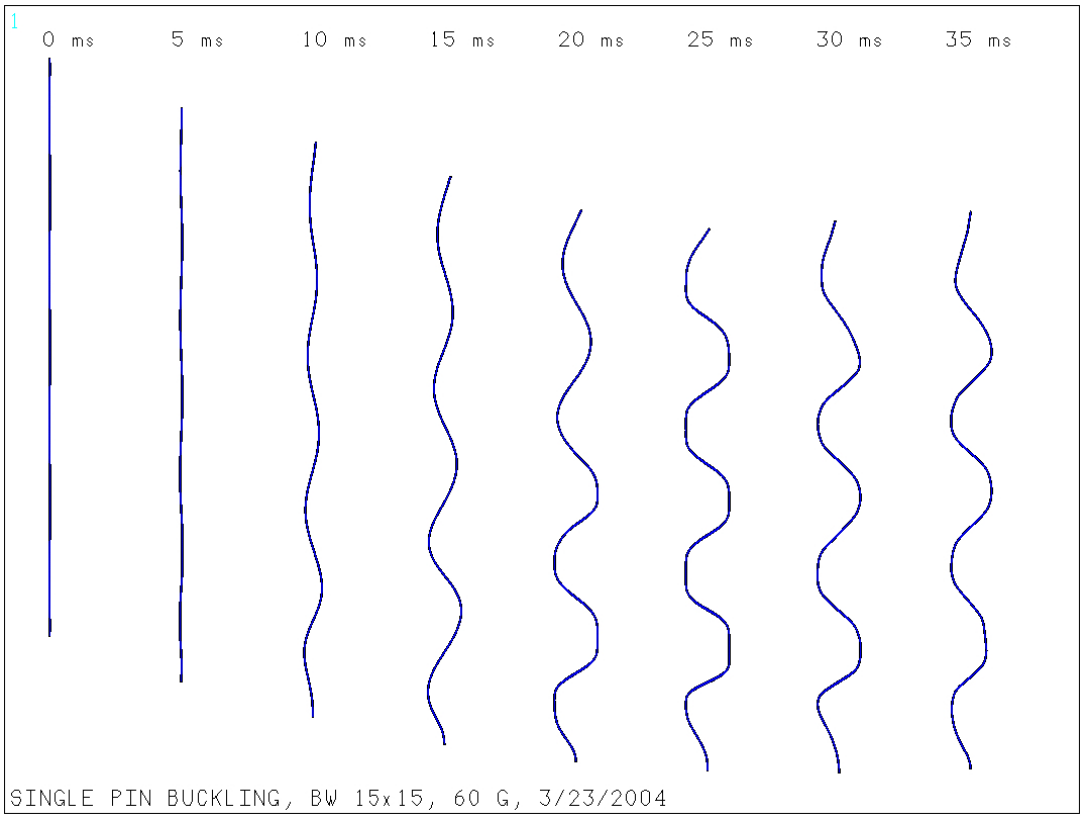

Figure 3. Deformed pin shape as a function of time.

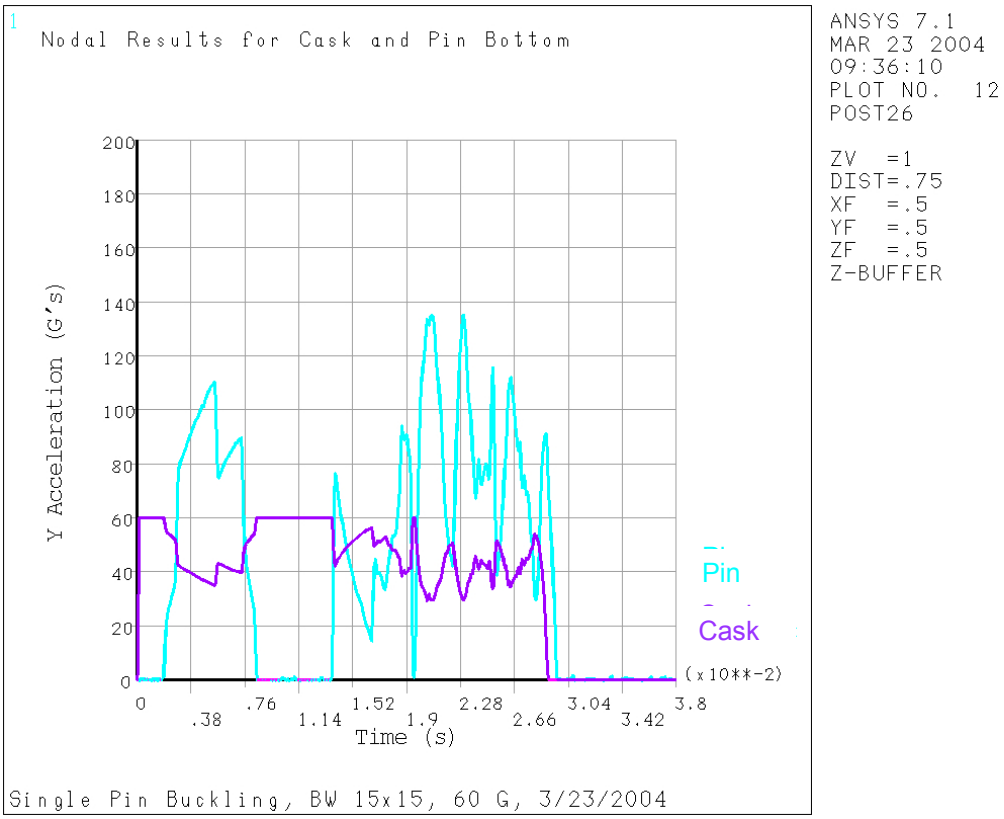

Figure 4. Cask and pin axial deceleration history.

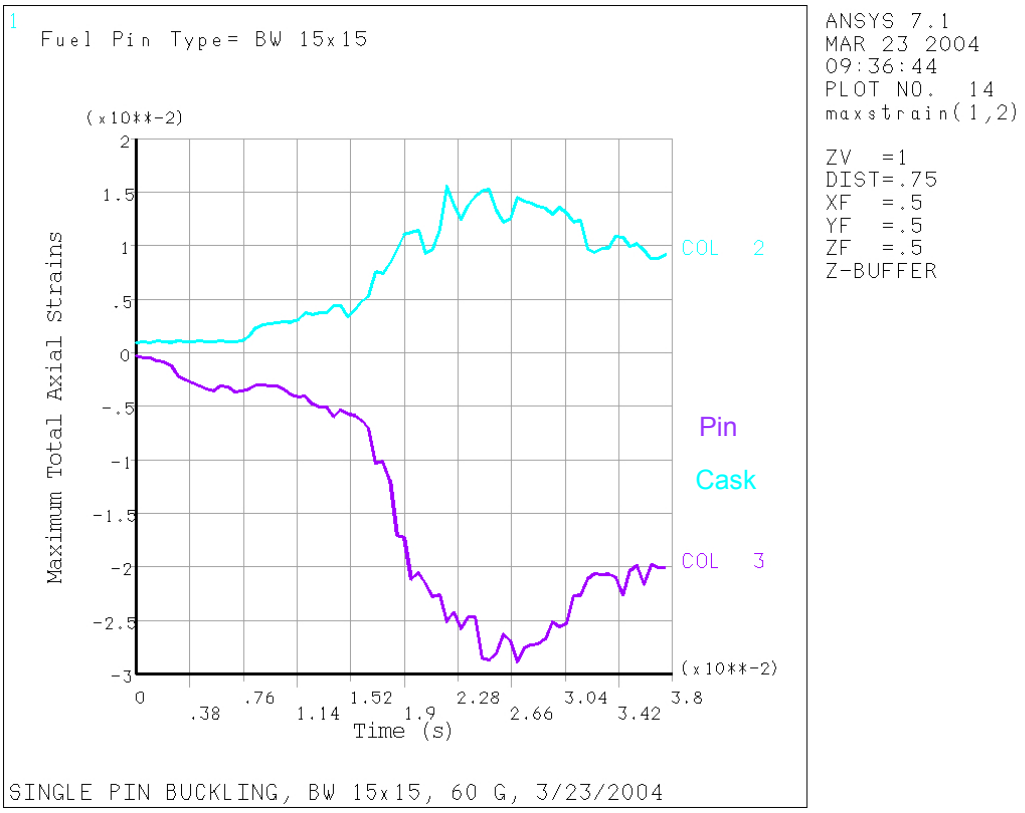

Figure 5. Peak cladding axial strain history.

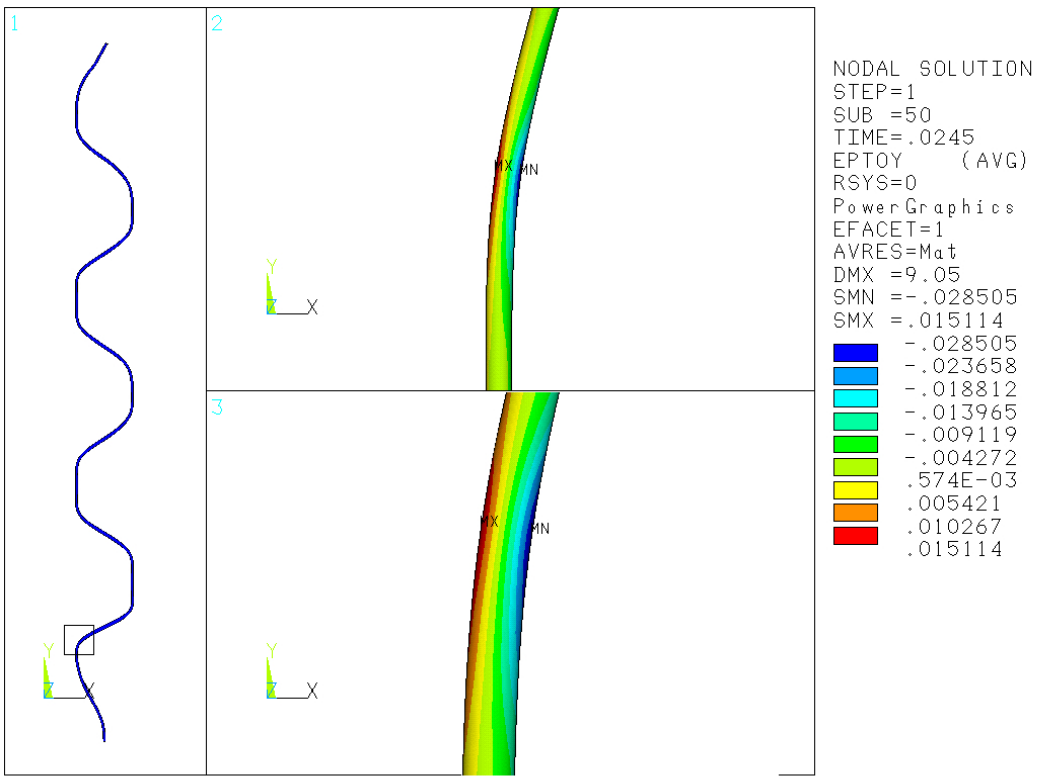

Figure 6. Peak cladding axial strain (t=24.5 ms).

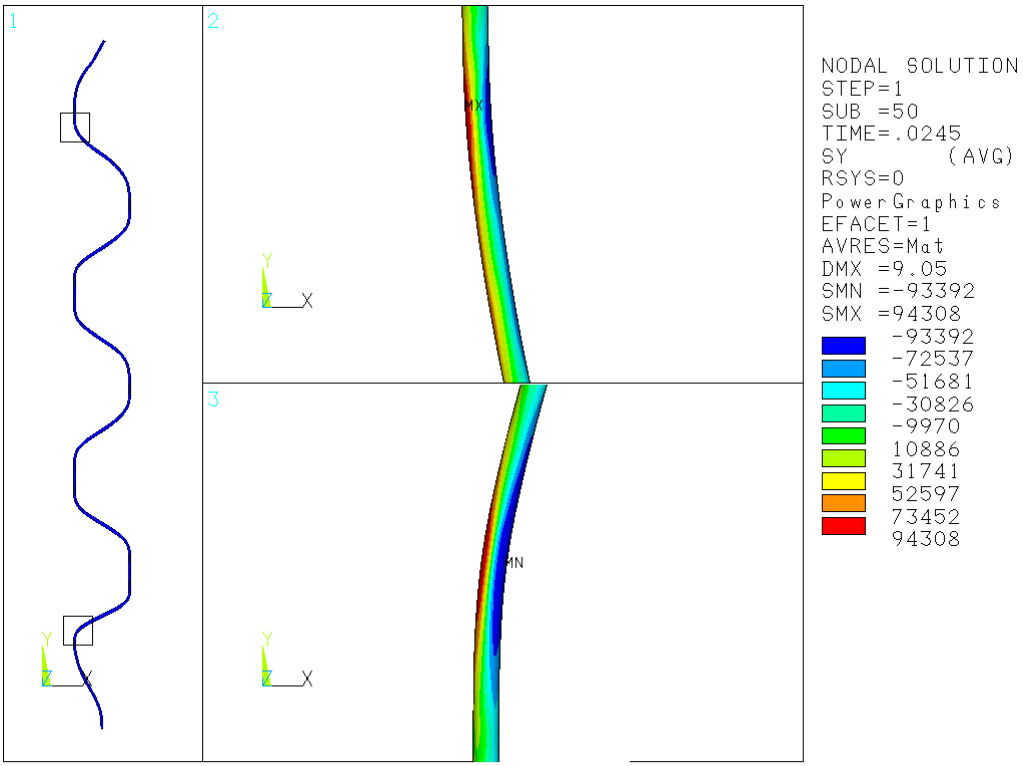

Figure 7. Peak cladding axial stress (t = 24.5 ms).
(Stress reported in units of psi and 1 psi = 6895 Pa)

5.2. Effect of Internal Pressure (Case 2)

During reactor operations, fission gases are generated within a pin and increase internal pressurization. For these analyses which include nonlinear material response for the cladding, loading due to pressurization generates additional stresses within the cladding. This could lead to the onset of plastic behavior and a lower buckling capacity. By comparing the results reported in Table 1 for Case 1 and Case 2 it can be seen that the internal pressurization causes the axial strains to increase for the same impact conditions. The tensile strain, which is relevant to pin fracture, increased from 0.8% to 1.5%. This meansimplies that internal pressurization should be considered in the nonlinear buckling analyses or any failure assessment.

5.3. Effect of Cask Deceleration (Case 3-4)

The influence of the average deceleration on the pin is intuitive. A minimum deceleration is required to cause buckling. Higher decelerations are expected to cause higher lateral crushing loads on the buckled pin and may even cause additional buckling modes in the unsupported regions of the pin. To assess the influence of acceleration loading, cases of 50 G's (Case 3) and 70 G's (Case 4) were also run to compare with the 60- G's baseline case. In both cases, buckling still initiated and the maximum pin deceleration changed as expected. For a 10 -G change in overall system deceleration, the maximum pin deceleration dropped 17 Gs for Case 3 and increased 28 Gs for Case 4. Similar behavior was observed with the strains. The strain magnitudes for the 50 -G case (Case 3) dropped approximately 20%, while larger increases of 25-71% were witnessed for the 70 -G case (Case 4). This suggests that the strains in Case 4 are higher due to increased lateral loading and pin flattening against the compartment wall.

5.4. Effect of Lateral Gap Width (Case 5-6)

When the pin buckles, it deforms laterally until it contacts the compartment walls and reaches a stable configuration. The lateral gap width between the pin and the wall dictate the geometry of this post-buckling configuration. Smaller gaps are assumed to be better, as large gaps generate large deformations and high bending strains. To assess the influence of the gap width, cases of 1.1" in (2.8 cm) and 1.3" in (3.3 cm) lateral gap were run to compare with the 1.2" in (3.05 cm) baseline case. The results indicated that strain magnitudes were reduced with a smaller gap (Case 5) and increased with the larger gap (Case 6) as expected, while maximum pin decelerations increased with a smaller gap and decreased with a larger gap. This indicates the smaller gap can withstand a higher maximum pin deceleration than the larger gap.

5.5. Effect of Cladding Reduction (Cases 7-8)

The critical buckling load for a pin depends on the area moment of inertia of its cross-section. If the wall thickness of the cladding is reduced, the buckling load is reduced. The cladding sectional rigidity under lateral loading is also reduced, so post-buckling deformations are more susceptible to fuel cladding ovalization during pin stack up against the compartment wall. A thinner cross-section is disadvantageous from a buckling standpoint.

The cross-sectional properties are expected to change due to formation of hydrides on the exterior of the fuel cladding. The hydrided layer is more brittle and will likely be fractured. This may also lead to a loss of material. To assess the potential loss of material and property degradation, two cases were run to reduce the outer diameter of the pin. This is analogous to assuming that the hydrided layer has no structural contribution. Ongoing research at PNNL suggests that the hydriding depth could range as high as 20% of the wall thickness (averaged about the circumference), so cases for 10% and 20% thickness reduction were performed. While the stiffness contribution was reduced, the full cladding mass was still incorporated. The results indicated that reduced cladding thickness was detrimental and tensile strains increased from 1.5% to 2.0-2.3% and compressive strains increased from 2.98% to 5.5-6.3%. Additional modeling had indicated that even greater thickness reductions caused secondary buckling events to occur. Therefore, a highly flexible cross-section is obviously not desirable as it could lead to fuel pin collapse within the compartment.

5.6. WE 17x17 Results (Cases 9-11)

In addition to the baseline fuel pin, results were obtained for a Westinghouse (WE) 17x17 Optimized Fuel Assembly (OFA) pin to assess the influence of pin geometry. This pin is also considered to be one on the lower end of the spectrum regarding margin of safety under buckling behavior with its smaller diameter and wall thickness. Cases were run for 50, 60, and 70 G's while preserving the other geometric and loading characteristics from the baseline case. The results indicated that the strain magnitudes are higher than those for the B&W 15x15. This smaller pin is much more flexible and exhibits significant flattening against the compartment wall. At 60 G's (Case 10), the

strains were 2.4% tensile and 5.6% compressive, which are approximately double that of the baseline. Therefore, this pin is a more limiting case than the baseline. The strains also increased with the increase of overall system deceleration as expected.

5.7. Effect of Including Fuel Cross-Section (Case 12)

The model used for the sensitivity analyses is based on the primary conservative assumption that the fuel contributes only mass effects and no flexural rigidity to the pin buckling behavior. The primary reason for this assumption is that the pellet/cladding interface is extremely complicated to characterize conservatively and very little information exists. If the strains in the simplified model were within acceptable limits regarding applicable failure modes, this model would solidly insure the integrity of the cladding material. However, the strains witnessed in many of these cases are in the range where potential failure of high burn-up cladding materials cannot be clearly ruled out.

To assess the influence of the fuel's flexural rigidity on the buckling response, this case includes a full representation of the fuel pellets. This model is not conservative. The pellets are assumed to be fully intact and fully adhered to the cladding and adjacent pellets. The fuel is given elastic material properties for UO_2 and no internal pressurization is included. While clearly not conservative in predicting post-buckling capacity, this case does provide a bounding scenario for the pin.

Using the B&W 15x15 assembly and the baseline conditions of Case 1, the results indicated that the pin would not buckle. The added flexural rigidity prevented the initiation of buckling, and the pin exhibited a response characteristic of elastic stress wave propagation in a long bar. The resulting strains were essentially elastic due to axial loading and some bending of the initially curved fuel pin. This result is not unexpected, but it reemphasizes the importance of the fuel contribution and its influence on axial impact loading. Even if the fuel is highly fractured within the confinement of the cladding, it is still expected to provide stiffening to the pin. Some method of pellet representation will need to be included in the modeling effort to obtain a more realistic estimate of fuel pin response.

5.8. Effect of Basket Geometry (Case 13)

The cask mass per pin is significantlyabout four times greater than the pin mass itself by a factor of four in the baseline case. This means that the cask has a great influence on the system dynamics during impact. BBy assuming a 24 assembly basket instead of a 32 assembly basket, the cask mass per pin is increased to about six times the individual pin mass. The effect of this larger relative cask mass is that theseen to cause larger pin deceleration must be greater for the same system deceleration. In this case, the pin deceleration increased slightly from 135 to 151 G's. There was also a corresponding increase of the compressive cladding strain to 3.3%.

5.9. Effect of Ramped Loading (Case 14)

For the baseline case, the impact limiter response is assumed to exhibit a uniform force-deflection response. This causes the system deceleration to be constant during the impact event. This assumption is the simplest estimate of impact limiter response, but the response of current designs may be different. Experimental data for representative impact limiters indicates that the total crush force tends to ramp up to its maximum value. Overall, this would tend to reduce initial decelerations and slow the response of the system. To determine the effect on the pin loading and provide a more realistic response, this case was run with a ramped force-deflection curve. The crush force was increased from zero0.0 to the assumed nominal value over a displacement of 10 in (25.4 cm).0".

Two effects were noted for the ramped loading. First, the impact duration is increased from a total of 29 ms to 38 ms. Second, prior to 22 ms at which time the full crush strength is obtained in the impact limiter, the pin accelerations are reduced. The initial deceleration maximum prior to buckling was reduced from 112 G's to 60 G's, and the overall peak deceleration was reduced from 135 G's to 126 G's. The peak cladding strains were just slightly smaller as they occurred after the impact limiter reached full crush strength.

6. Conclusions

For the models with no fuel pellet contribution to flexural rigidity, the resulting tensile axial strains in the cladding ranged from 0.8% to 2.7% depending on the geometry analyzed. A conservative baseline case, which discounted the contribution of the fuel pellets to the pin's flexural rigidity and at the same time considered 100% of their mass contribution, yielded peak tensile and compressive strain magnitudes of 0.015 in/in and 0.028 (in/in (or 1.5% and

2.8%), respectively. A limiting case involving full contribution of fuel pellets to flexural rigidity yielded peak tensile and compressive strain magnitudes of 0.00066 in/in and 0.00082 in/in (or 0.066% and 0.082% strain), respectively.

Permissible strains regarding failure mechanisms for high burn-up fuels are difficult to determine due to limited data, but ongoing work at PNNL has estimated that they are on the order of 1.0 to 2.8%. The analytical results from the baseline evaluation case are on the order of this estimated material limit. Clearly, results from this conservative baseline evaluation should not be interpreted as actual fuel assembly behavior. It provides insights to potential structural behavior of high burnup fuel with expert input on mechanical fuel properties. However, the analyses demonstrated that buckling would not occur and strains were very low when the fuel pellet flexural rigidity was fully accounted for and perfect bonding was assumed at the cladding-fuel pellet interface.Permissible strains regarding failure mechanisms for high burn-up fuels are difficult to determine due to limited data, but ongoing work at PNNL has estimated that they are on the order of 1.0 to 2.8%. The analytical results from the baseline evaluation case are on the order of this estimated material limit. Clearly, results from this conservative baseline evaluation do not provide sufficient evidence that cladding failure cannot happen during end impacts typically experienced in a drop accident event (as defined by 10CFR71.73[3]). However, buckling did not occur and strains were very low when the fuel pellet flexural rigidity was fully accounted for and perfect bonding was assumed at the cladding-fuel pellet interface.

Since the strains yielded by the baseline evaluation model were nearly at an acceptable magnitude with the conservative assumption of neglecting fuel pellet flexural rigidity, a high degree of confidence regarding cladding survival is still expected. The assumptions inherent to the single pin model will be addressed further with a cask-fuel assembly model including 3D pin deformations, pin-pin interactions, improved spacer grid representation, and more detailed modeling of the fuel effects.

7. Acknowledgments

The authors would like to thank Carl Beyer of PNNL for his contributions and assistance regarding high burn-up spent fuel material properties. The authors would also like to thank Gordon Bjorkman, of the USNRC, for his insightful comments and contributions on this study. Pacific Northwest National Laboratory is operated by Battelle for the U.S. Department of Energy under Contract DE-AC06-76RL01830.

8. References

[1] Title 10, Code of Federal Regulations, Part 71, Subpart 73, *Packaging and Transportation of Radioactive Material*. Jan. 1, 2003, United States Government Printing Office, Washington, DC.

ANSYS, Inc. 2003. "ANSYS®/LS-DYNA®TM User's Guide." in *ANSYS Release 7.1 Documentation*. Canonsburg, PA.

[2] ANSYS, Inc. 2003. "ANSYS®/LS-DYNA™ User's Guide." in *ANSYS Release 7.1 Documentation*. Canonsburg, PA. Sanders TL, KD Seager, YR Rashid, PR Barrett, AP Malinauskas, RE Einziger, H Jordan, TA Duffey, SH Sutherland, and PC Reardon. 1992. *A Method for Determining the Spent-Fuel Contribution to Transport Cask Containment Requirements*. SAND90-2406, Sandia National Laboratories, Albuquerque, NM.

[3] Sanders TL, KD Seager, YR Rashid, PR Barrett, AP Malinauskas, RE Einziger, H Jordan, TA Duffey, SH Sutherland, and PC Reardon. 1992. *A Method for Determining the Spent-Fuel Contribution to Transport Cask Containment Requirements*. SAND90-2406, Sandia National Laboratories, Albuquerque, NM.

Title 10, Code of Federal Regulations, Part 71, Subpart 73, *Packaging and Transportation of Radioactive Material*. Jan. 1, 2003, United States Government Printing Office, Washington, DC.

[4] Bjorkman GS. April 2004. "*The Buckling of Fuel Rods in Transportation Casks Under Hypothetical Accident Conditions.*" Proceedings of Twelfth International Conference on Nuclear Engineering, ICONE12-49554, Arlington VA.

[5] US Nuclear Regulatory Commission (USNRC). 1999. *Buckling of Irradiated Fuel Under Bottom End Drop Conditions.* ISG 12 Rev 1, Washington, DC.

[64] Electric Power Research Institute (EPRI). 1991. *Fuel-Assembly Behavior Under Dynamic Impact Loads Due to Dry-Storage Cask Mishandling*. EPRI-NP-7419, prepared by ABB Combustion Engineering, Inc. for Electric Power Research Institute, Palo Alto, CA.

[7] Roark RJ. 1965. *Formulas for Stress and Strain*, 4th ed. McGraw-Hill, New York.

[85] Adkins HE, BJ Koeppel, and DT Tang. 2004. "Spent Nuclear Fuel Structural Response When Subject to an

End Impact Accident." in proceedings of the 2004 ASME/JSME Pressure Vessels and Piping Division Conference, *Transportation, Storage and Disposal of Radioactive Materials*, ed. AC Smith and R Hafner, PVP-Vol. 483, ASME, Fairfield, NJ.

Harold E. Adkins, Jr.
Fluid and Computational Engineering Group
Pacific Northwest
National Laboratory
Richland, WA
(509) 372-6629
harold.adkins@pnl.gov

Brian J. Koeppel
Computational Mechanics Group
Pacific Northwest
National Laboratory
Richland, WA
(509) 372-6816
brian.koeppel@pnl.gov

David T. Tang
Spent Fuel Project Office
U.S. Nuclear Regulatory Commission
Washington, D.C.
(301) 415-8535
dtt@nrc.gov

[6] Roark RJ. 1965. *Formulas for Stress and Strain*, 4th ed. McGraw-Hill, New York.

Abstract
The U.S. Nuclear Regulatory Commission (USNRC) is tasked with licensing of safe spent fuel storage and transportation systems. A subset of this responsibility is to investigate and understand the structural performance of these systems. In a joint effort between staff at the Pacific Northwest National Laboratory (PNNL) and the USNRC, computational studies were performed to predict the structural response of spent nuclear fuel when subject to an end impact accident. In this study the structural performance of a typical pressurized water reactor (PWR) fuel assembly is evaluated utilizsing the ANSYS®/LS-DYNA®[1] finite element analysis (FEA) code.

introduction
A renewed interest in examining more closely the structural integrity of fuel pins under storage handling and hypothetical transportation accident conditions has arisen from a recent initiative to store and transport high- burn-up (45- to 75 GWd/MTU) fuels. Cladding failure may assume a variety of modes depending on loading conditions, fuel geometry, and material properties. It was found in the report SAND90-2406,[2], in general, that the pressurized water reactor (PWR) fuel cladding was more vulnerable to impact events than the boiling water reactor (BWR) cladding. For the axial loading and inelastic buckling of a representative PWR fuel pin, at a prescribed 100 -G G acceleration, the report computed maximum bending strains of approximately 2% with lateral restraint and 8% at incipient collapse without lateral restraint.
Experimental tests are in the process of being conducted to generate mechanical property and toughness data for high- burn-up fuel cladding materials. Based on information to date, uniform elongation (ductility) of high burn-up fuel cladding is anticipated to range from 1.7%% to over 3.0%. This is the same order of magnitude as that previously calculated by Sandia National Laboratories.[2].
Simulation Approach
The main objective of this study was to use a numerical model to compute the inelastic buckling capacity and corresponding strain ductility demands for a representative spent fuel assembly pin under a simulated cask handling or drop accident as defined in Code of Federal Regulations, Title 10, Part 71, Subpart 73 (10CFR71.73).[3]. In this study, an explicit finite element analysis (FEA) model of a single pin, with lateral displacement constraints, is developed for evaluating fuel pins subject to end impact loads. The scope of the analyseis involves cask impact accelerations of 60 G's, a total assembly-to-compartment gap of 0.325" in. (0.826 cm), an internal pin pressure of 1400 psi (9.65 MPa), and a Babcock & Wilcox (B&W) 15x15 pin geometry. Two separate models for the fuel pellet stiffness effects are considered in this study. The first "baseline" case serves as a conservative evaluation by discounting the contribution of the fuel pellets to the pin's flexural rigidity but still considering 100% of their mass contribution as demonstrated analytically by Bjorkman[4] and recommended by the USNRC.[5]. The second "limiting" case examines the same pin with contribution of the fuel cross-section for flexural rigidity of the pin.
ANSYS® was used in this study for general model development, whereas the explicit solution was performed by LS-DYNA®. The LS-DYNA® solver was accessed and utilizsed through its existing implementation in the ANSYS® framework. While the impact event entails the interaction of hundreds of pins, their spacer grids, tie plates, fuel spacers, basket, cask, and impact limiters under dynamic loading, for computational efficiency it is desirable to model a single pin as was done in some previous studies.[2,6]. This model considered the following assumptions:

1.**All pins deform in the same shape**. It was assumed that all the individual pins of a fuel assembly would impact and displace with the same deformed shape. This suggests that the single -pin response is characteristic of all pins and can be studied independently.. This is It also assuminges that the center pin in the assembly is

representative of the typical response of the cross -section of pins through the whole assembly, and that the control pins behave like a typical pin within the assembly.
2.Pin deformation is planar. It was assumed that all bending deformations occurred in a single plane, although an actual assembly could exhibit bending deflections and/or twisting within the fuel compartment. This assumption allowed only half of the pin to be modeled.
3.Fuel pellets provide partial structural influence. The 3D FEA model uses a shell element to model the mass and stiffness properties of the cladding cross section, but for the baseline case, no comparable representation of the fuel was included. This assumption, which is consistent with common fuel pin buckling analysis, was selected to yield a conservative reference point by discounting the contribution of the fuel pellets to the pin's flexural rigidity but still considering 100% of their mass contribution. However, to overcome unrealistic ovalization of the open cross-section, nonlinear single degree-of-freedom springs were included to represent a Hertzian-type radial contact between the cladding and the fuel during lateral loading.
4.Fuel pins are initially bowed. Spent fuel pins will typically exhibit deviations from straightness after exposure to a neutron flux.[2]. For pins mounted within an assembly using spacer grids, the unsupported sections of pin tend to bow out. Accordingly, a small amount of pin bowing was introduced to facilitate computation of fuel pin capacity.
5.Spacer grids provide lateral support only. The spacer grids are composed of a small array of leaf springs that hold the pins within the assembly. The spacer grid springs are assumed to provide lateral support to the pins with a prescribed nonlinear force-deflection curve. No rotational support is accounted for, and the grids cannot slide axially relative to the pin.
6.Cask modeled as a point mass. The cask was included in the model to capture pin-cask dynamics. This was implemented by defining a point mass to represent the cask (equal to the total physical mass of the packaging system divided by the total number of pins accommodated).
7.Impact limiter exhibits constant force-deflection characteristics. The impact limiter absorbs energy using a constant force-deflection curve whose magnitude is determined by the product of the impact limiter cross- sectional area and characteristic crush strength. This means the cask-pin system will experience a constant deceleration with no impact limiter "lock-up."
Model Geometry and Meshing
A drawing of the model representation for the single pin model is shown in Figure 1Figure 1Figure 1. It is composed of a single fuel pin, a lumped cask mass, springs representing the spacer grids, contact surfaces representing the compartment wall, and a spring representing the impact limiter. Several views of the actual finite element mesh are shown in Figure 2. In this figure, the views shown are a) the entire model, b) top of pin with compartment walls and spacer grid spring, c) top of pin with fuel pellet springs, and d) bottom of pin with nodes representing cask and impact limiter bodies.

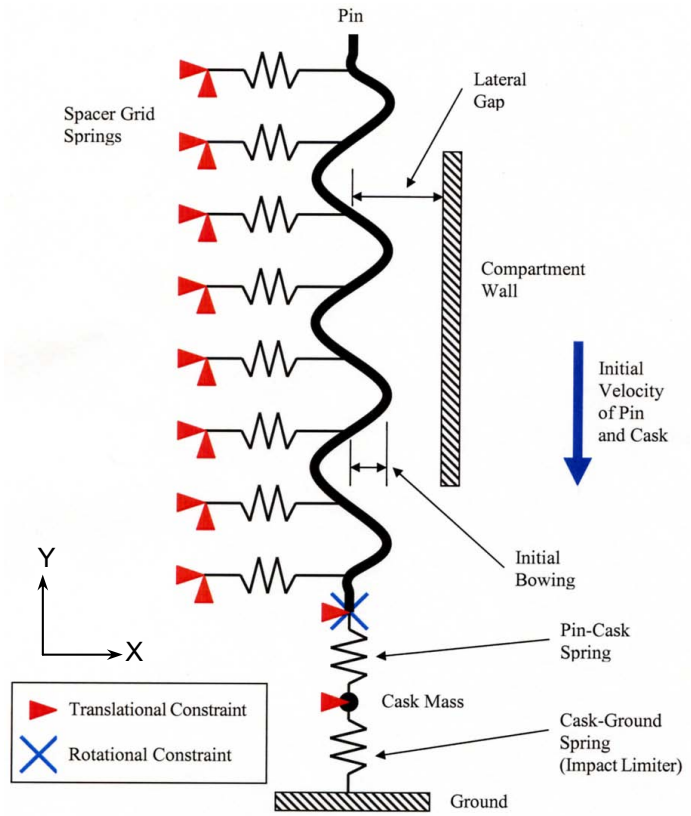

Figure 1. Schematic of model geometry and boundary conditions.

a lumped cask mass, springs representing the spacer grids, contact surfaces representing the compartment wall, and a spring representing the impact limiter. Several views of the actual finite element mesh are shown in . In this figure, the views shown are a) the entire model, b) top of pin with compartment walls and spacer grid spring, c) top of pin with fuel pellet springs, and d) bottom of pin with nodes representing cask and impact limiter bodies.

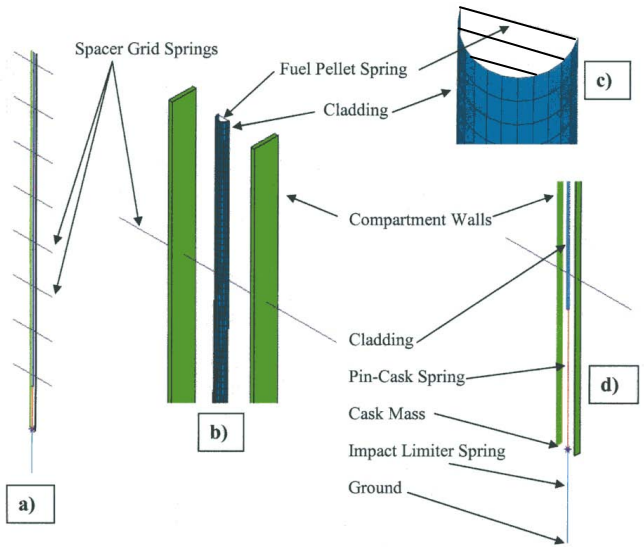

Figure 2. Finite element model for the single -pin analysis.

The typical fuel assembly pin is composed of cylindrical fuel pellets within a tubular cladding material that has reinforced end thimbles and an internal spring to minimize the gap between the fuel pellets at all times. The pin was modeled using shell elements with appropriate thickness and diameter to represent the cladding, and included about 20,000 elements and 10,000 nodes. The element sizing provided sufficient resolution for the stress state.

Fuel Pin

The pin was modeled with an initial bowed geometry of 0.071” in (0.180 cm) between the spacer grids.[2]. It was assumed that the pin had an initial constant curvature in these sections. At the pin ends, it was assumed that they had no initial rotation and that this condition would exist due to the constraint provided by the upper and lower tie plates.

Spacer Grids

The spacer grids are arrayed structures that provide intermediate support to the fuel pins in the assembly. The grids are composed of small leaf springs that ensure proper spacing of the pins in the assembly array. The grids were assumed to provide lateral support to the pin at eight intermediate locations (Figure 1Figure 1Figure 1) according to the fuel geometry considered. This contribution was represented by sets of compression-only springs attached to each side of the cladding cross- section. These springs behave such that a lateral pin deflection will compress one spring and generate a compressive force, while the spring on other side is unloaded to simulate loss of contact.

Fuel Compartment

Deflection of the fuel pins during an impact event will lead to pin-to-pin and pin-to-compartment wall contact. For an assembly with all pins deforming identically, the outer pins will be the first to contact the compartment walls. Additional deformation causes the next set of pins to seat against these outer pins. This stacking continues until all pins are compressed against the compartment wall. To implement this behavior in a single- pin model, the total lateral distance over which a pin could deform must be determined. The gap was determined by considering the pin diameter, number of pins, and compartment width to determine the total free space in which the center pins in an assembly could unilaterally deform. The lateral gap on each side of the center pin is given by

$$gap = \left(\frac{W_{compartment} - n_{pin} D_{pin}}{2} \right)$$

where

Wcompartment - inner width of fuel compartment

npin - number of pins across an assembly

Dpin - outer diameter of pin.

The compartment walls were then modeled as rigid planes fixed in space at the proper lateral gap (Figure 2Figure 2Figure 2). Contact elements were implemented to automatically capture contact between the cladding and the compartment walls.

Pin-Cask-Impact Limiter Interaction

Analyses indicated that the cask and impact limiter contributed significantly to pin dynamics, as expected. To include the effects of cask mass on system dynamics, the cask was modeled as a point mass. A compression-only spring was then used between the pin bottom and the cask. A second compression-only spring was then used to simulate the impact limiter and ground contact,, where the ground was assumed to be rigid. This model setup permitted the system to impact the target surface; however, any rebounding and loss of contact between the pin and the cask or the cask and the ground would be captured.

Material Properties

Cladding

The temperature-dependent material properties for the Zircaloy cladding material were obtained from PNNL research on a companion project to estimate mechanical properties of high- burn-up fuels. A uniform temperature of 500°F (260°C) was assumed for the pin, and the corresponding material property estimates were:

Elastic Modulus = 10.98e6 psi (75.7 GPa)
Yield Strength = 92.4e3 psi (637.1 MPa)
Tensile Strength = 94.4e3 psi (650.9 MPa)
Tensile Strain = 2.35%
Poisson’s Ratio = 0.404.

These values were used to generate athe stress-strain curve as shown in Figure 3Figure 3Figure 3. The material was given a perfectly plastic response beyond the tensile strain value for computational simplicity. An effective density was computed directly from the reference mass per pin and the total cladding volume in the model.

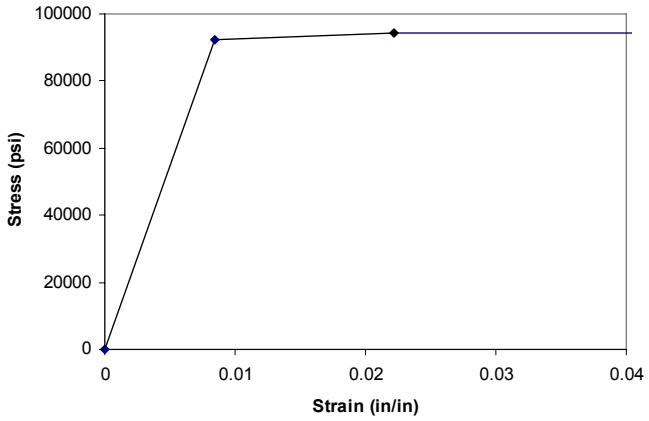

Figure 3. Estimated material response curve for Zircaloy cladding.

Fuel Pellet Spring

To simulate the fuel-clad interaction and its ability to limit gross cladding ovalization, the fuel pellet was modeled as an equivalent spring function. The force-deflection curve for this spring was adapted from the solution of an elastic cylinder under Hertzian contact between two plates as defined inby Roark.[7]. The resulting force-deflection curve and spring stiffness is shown in Figure 4Figure 4Figure 4.

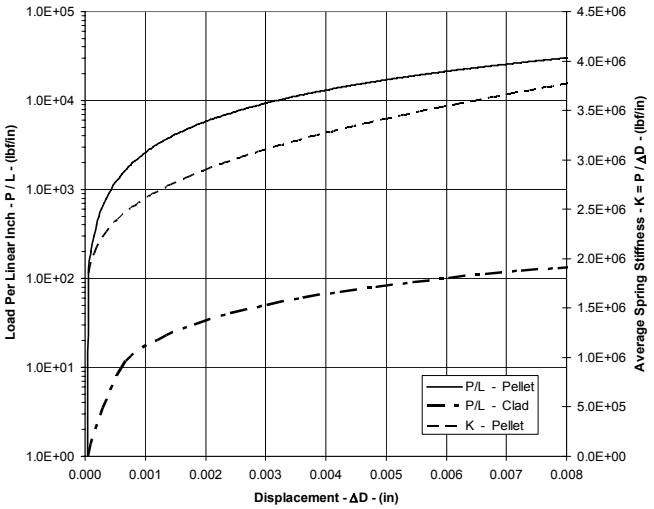

Figure 4. Fuel pellet spring load and stiffness curves as a function of displacement.

Spacer Grid Spring

The force-deflection curves for the spacer grid springs were taken from Sanders.[2]. These numbers are assumed to be adequate for this modeling effort and eliminated the need to generate new curves via analysis. The curves represent elastic deformations from a number of compounding events during the lateral compression of a fuel assembly, including 1) compression of the spacer grid leaf spring, 2) compression of the spacer grid frame, 3) buckling of consecutive spacer grid cells, and 4) crushing of the fuel pin cross- section. The spacer grids at the top and bottom of the assembly are attached to the end plates and are consequently stiffer, so they are represented by a different curve. The resulting force-deflection curves for the middle and end spacer grids are shown in Figure 5Figure 5Figure 5.

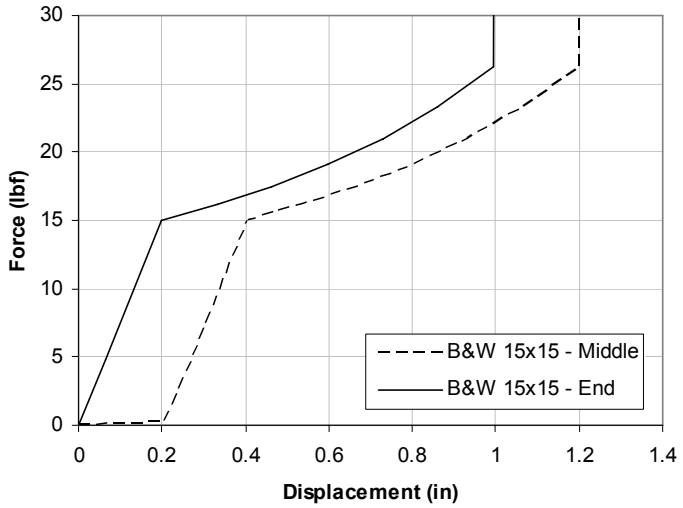

Figure 5. Fuel assembly spacer grid spring load-deflection curves.

Pin-Cask Spring

The pin-cask spring represents the interaction between the bottom of the pin and the tie plate as they are driven together during the impact process. A value of 1e5 lb/in (1.75e5 N/cm) was selected for the stiffness after sensitivity analyses.

Cask-Ground Spring

The cask-ground spring represents the behavior of the impact limiter. This is the major source of energy absorption in the system. The impact limiter is characterized by constant force deflection, where the force magnitude is defined by the product of the impact limiter area and the material crush strength. The spring is compression-only to permit the cask to lose contact with the ground when it rebounds. The unloading of the spring occurs with the same modulus as during loading to simulate the non-recoverable crushing behavior of the honey-comb. The load-deflection curve for the spring representing the impact limiter is shown in Figure 6Figure 6Figure 6 (slope of the unloading curve remains as shown but can occur at any deflection depending on the loading involved). The assumed properties and resulting crush forces are:

Elastic Modulus = 400 ksi (2.76 GPa)
Crush Strength = 1050 psi (7.24 MPa)
Impact Limiter Diameter = 128 in (325 cm)
Crush Force = 1050*π/4*1282 = 13.5e6 lb (6.0e7 N)
Crush Force/Pin = 13.5e6/(15*15*32) = 1875 lb (8340 N).

This crush force then dictates the average deceleration values for the system components. For example, a system with an assumed loaded cask weight of 275,000 lb has an average deceleration of:

Overall System Deceleration = 13.5e6/275000 = 49 G's

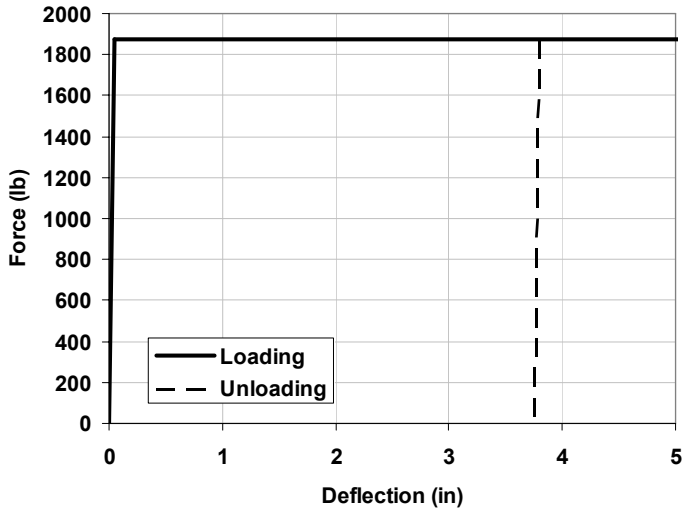

Figure 6. Impact Limiter spring load-deflection curve.

Boundary and Initial Conditions

The boundary and initial conditions for the model are summarized below:

- Out-of-plane translations and rotations were constrained along the symmetry plane of the pin.
- In-plane rotation and lateral translation was constrained at the bottom of the pin. This is based on the assumption that the pins will likely be "jammed" into the bottom tie -plate and restrict rotation and lateral translation.
- Vertical translation only was enforced for the pin-cask spring, cask, and cask-ground spring.
- All translations were fixed for the free ends of the spacer grid springs.
- All translations were fixed for the ground surface.
- An initial velocity of 528 in/sec (1341 cm/s) (corresponding to the standard regulatory 30 ft (9.1) drop – 10CFR71.73[3]) was applied to the pin and cask nodes.

Loading

After a fuel assembly has been exposed to a neutron flux and burned for high -burn-up durations (>45 GWd/MTU), internal pin pressures due to fission gas generation can range from 1000 to 2200 psi (6.89 to 15.16 MPa). A pressure loading of 1400 psi (9.65 MPa) was applied to the inner cladding surface to simulate the effects of this fission gas generation. This was applied as a preload to the system using a stress initialization procedure prior to solution of the impact event.

Simulation Results

Baseline Case

The standard width of the PWR assemblies selected for this study is 8.43" in (21.4 cm) square. The standard fuel compartment width (Wcompartment as defined above) selected for this study is 8.75" in (22.2 cm) square and is considered typical.

The baseline case is performed with the B&W 15x15 fuel assembly pin geometry. Characteristic dimensions for this pin include a cladding thickness of 0.0265" in (0.0673 cm), an outer diameter of 0.429 in" (1.09 cm), and an overall length of 153.7" in (390.4 cm). The total weight of this pin is 7.011 lbs (3.183 kg). Other inputs selected for this case are a loaded cask weight of 275,000 lb (124,850 kg), an average deceleration of 60 G''s for the cask mass, a total assembly-to-compartment wall lateral gap of 0.325" in (0.826 cm) (which equates in the model to a 1.2" in (3.048 cm) lateral gap on either side of the center pin when all gaps between pins are incorporated), internal pressurization of 1400 psi (9.65 MPa), and cask loading with 32 assemblies. These values are representative of typical transport cask systems in use.

Presented in Figure 7Figure 7Figure 7 is a series of exaggerated deformed shapes of the assembly pin as the impact event progresses from initiation to rebound. Deformed shapes are presented for time starting at 0 ms (initiation) and plotted at intervals of 5 ms from left to right. As the impact event progresses, the pin initiates buckling and begins to deflect laterally. Where the pin is held by the stiff spacer grid springs, the pin deflects very little and remains near the center of the enclosure. The large lateral deflections occur in the unsupported regions, and the deflection direction alternates for each region (creating the expected sinusoidal-like deformation). This zonal lateral deflection continues until the pin reaches the contact surfaces representing its surrounding fuel pins fully deflected and against the fuel compartment wall.

As the event progresses further, the long unsupported pin sections between spacer grids begin to flatten against the compartment wall, while the pin sections supported by the spacer grids remain at the center of the enclosure. As the flattened sections grow in length, the bending moment applied to the pin grows in the vicinity of the maximum curvature locations where the pin starts to contact the compartment wall. As the event continues and

nears completion, the pin unloads and begins to rebound. Following is a detailed description of the events that occur during the impact.

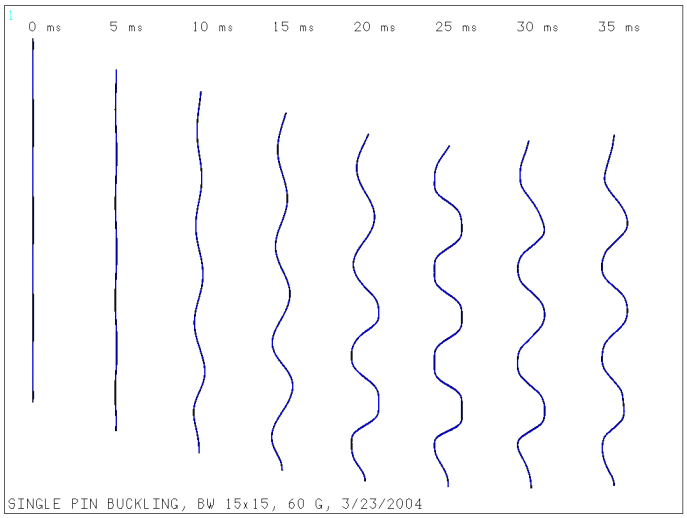

Figure 7. Deformed pin shape as a function of time.

As the event continues and nears completion, the pin unloads and begins to rebound. The following is a detailed description of the events that occur during the impact.

0 ms < t < 2 ms
Presented in Figure 8Figure 8Figure 8 through Figure 11Figure 11Figure 11 is a series of history plots featuring the rigid-body velocity of the assembly pin, comparative nodal results for axial displacement and velocity of the transport system (cask) and bottom of the assembly pin, and axial rigid-body accelerations for the pin and cask. As shown in these figures, from 0-2 ms, the cask node instantaneously contacts the ground and experiences a 60 G deceleration as dictated by the load deflection curve for the impact limiter spring. However, the pin is still traversing over an initial 0.040”-in (0.102 -cm) gap originally provided in the model between the cask and pin. This is apparent from the constant pin velocities featured in Figure 8Figure 8Figure 8 and Figure 10Figure 10Figure 10, and the constant accelerations featured in Figure 11Figure 11Figure 11 for this duration.
2 ms < t < 8 ms
At the beginning of this period, the fuel strikes the transport system and begins to influence its deceleration by assisting in impact limiter crush. Over this duration, the pin begins to rapidly decelerate and hits a peak deceleration of approximately 110 G’s while the cask’s deceleration is slightly reduced to approximately 36 G’s due to the interaction with the fuel assembly mass. This is shown in Figure 8Figure 8Figure 8 and Figure 11Figure 11Figure 11. As shown in Figure 10Figure 10Figure 10, the fuel and cask velocities are essentially the same over this period. Hence, the fuel assembly mass is maintainings contact with the transport system.
8 ms < t < 14 ms
Buckling instability of the fuel assembly pin initiates large lateral deflections in the pin until it makes contact with the compartment wall. Evidence of this is shown in Figure 8Figure 8Figure 8 and Figure 11Figure 11Figure 11. During this lateral collapse, the pin is unstable and will experience buckling deformations without bound and with no external force acting on it. As such, its rigid-body velocity becomes constant and the cask deceleration returns to its original magnitude over this duration.

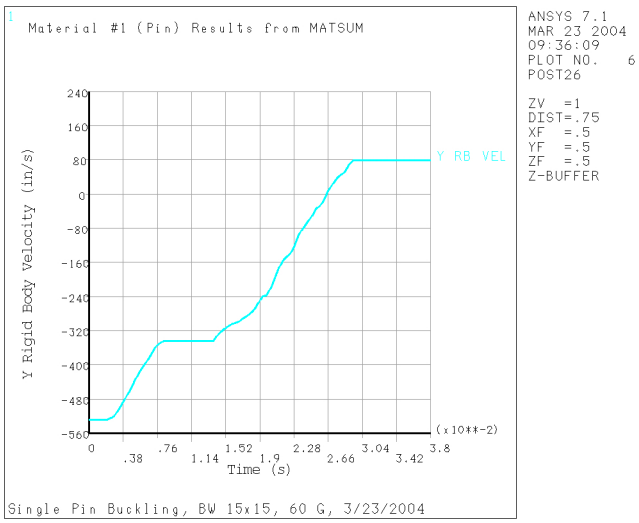

Figure 8. Pin rigid-body velocity history.

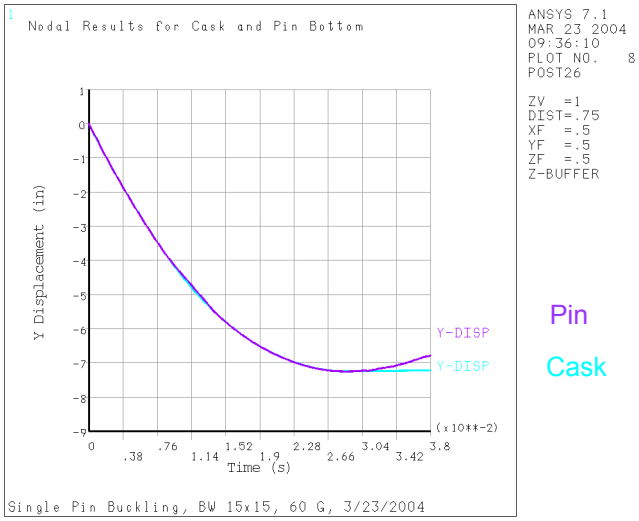

Figure 9. Cask and pin bottom axial displacement history.

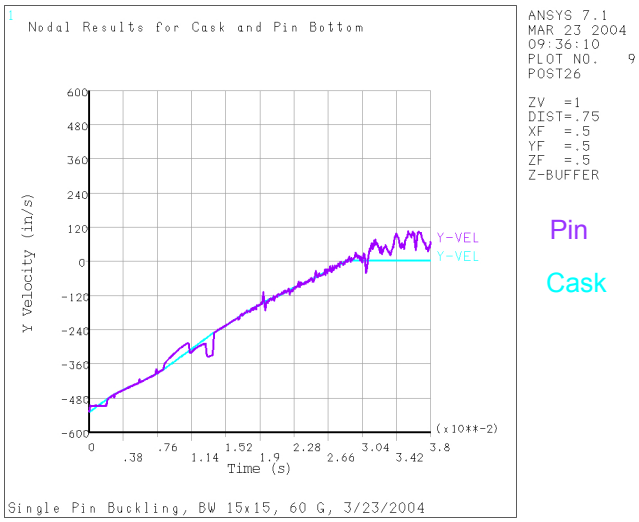

Figure 10. Cask and pin bottom axial velocity history.

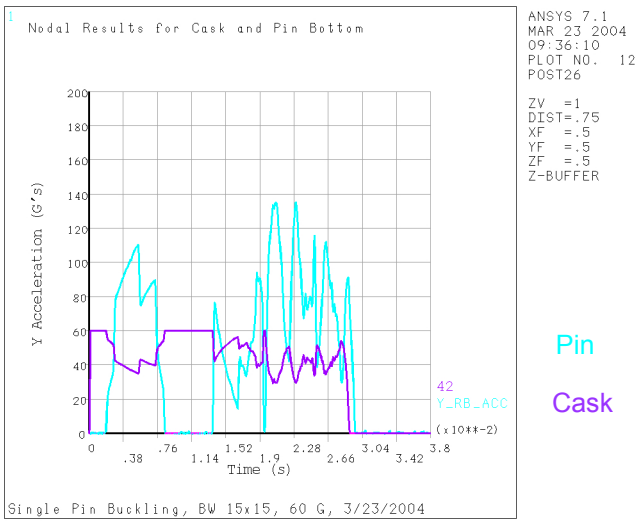

Figure 11. Cask and pin axial deceleration history.

During collapse, for this case, the assembly pin breaks contact with the cask mass for a brief moment. This is shown in the minor displacement difference between the two bodies in Figure 9Figure 9Figure 9 as well as the cask and pin bottom axial velocity history (Figure 10Figure 10Figure 10). Collapse continues until the extent of lateral deflection creates side contact. This post-buckling deformation is stable and will stiffen the pin structure for additional loading.

14 ms < t < 28 ms

At the beginning of this period, the fuel assembly pin has laterally deflected and made contact with the compartment wall. The fuel assembly is now fully seated against the bottom and wall of the compartment in a stable configuration and begins to once again influence the cask deceleration by participating in impact limiter crush. During this durationperiod, the pin is again rapidly decelerated with significant dynamic effects and reaches a peak deceleration of approximately 135 G's while the cask's deceleration is approximately 40 G's on average. This is due to the dynamic interaction between the fuel assembly and transport system body (Figure 11Figure 11Figure 11). Despite the high magnitude of deceleration that the fuel assembly pin is subjected to during this time range, the actual duration of the peaks is extremely short (~2 ms each).

28 ms < t < 38 ms

As shown in Figure 9Figure 9Figure 9 and Figure 10Figure 10Figure 10, the beginning of this period marks the end of the primary impact duration and the initiation of assembly (pin) rebound. At this point the loaded transport system has dissipated most of its kinetic energy through impact limiter crush. The pin is beginning to spring back away from the cask in an upward vertical direction (positive velocity and displacement difference), whereas the cask impact limiter has undergone an inelastic collision with the impact target and has a much smaller rebound velocity.

Overall Results

A rigid-body deceleration history was assembled for the entire package to verify proper overall deceleration characteristics. It and is shown in Figure 12Figure 12Figure 12. As shown, the magnitude for the entire system remains constant at 49 G's over the duration as expected from the constant crush strength of the impact limiter. Presented in Figure 13Figure 13Figure 13 is the global peak axial strain history for the pin, which is generated from the maximum instantaneous tensile and compressive axial strains anywhere in the cladding (i.e., the results are not from a single location). Despite the high magnitude of the peak pin deceleration (135 G's) (- Figure 11Figure 11Figure 11), the peak tensile and compressive strains only reach magnitudes of 0.015 in/in and 0.028 in/in (or 1.5% and 2.8%), respectively.

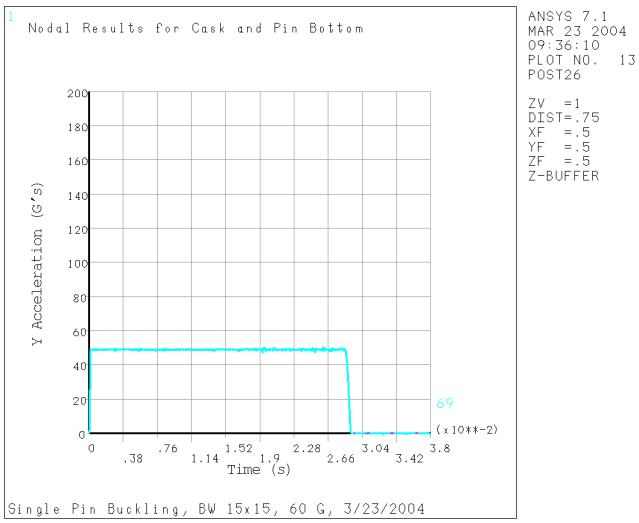

Figure 12. Package axial deceleration history.

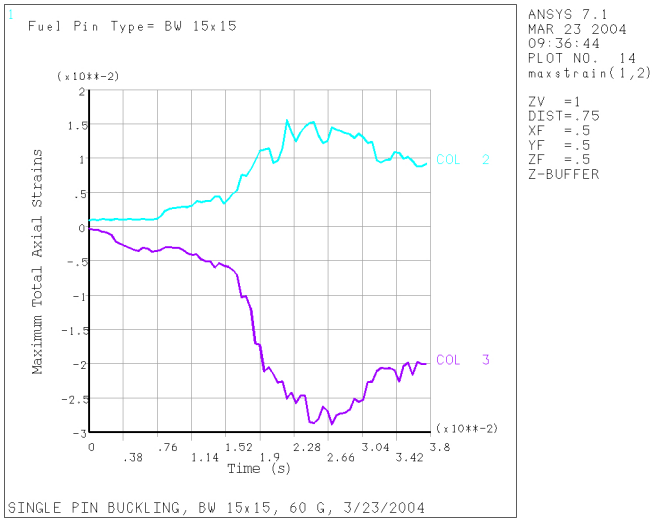

Figure 13. Peak cladding axial strain history.

Presented in Figure 14Figure 14Figure 14 and Figure 15Figure 15Figure 15 are the instantaneous total axial strains and stresses, respectively, for t = 24.5 ms. As discussed earlier, as the flattened sections grow in length, the bending moment applied to the pin grows in the vicinity of the locations where the pin breaks contact with the compartment wall. These locations yield the highest stresses and strains, which are shown to be very localized. It should be noted that the pin displacements in these figures have been exaggerated to display their behavior.

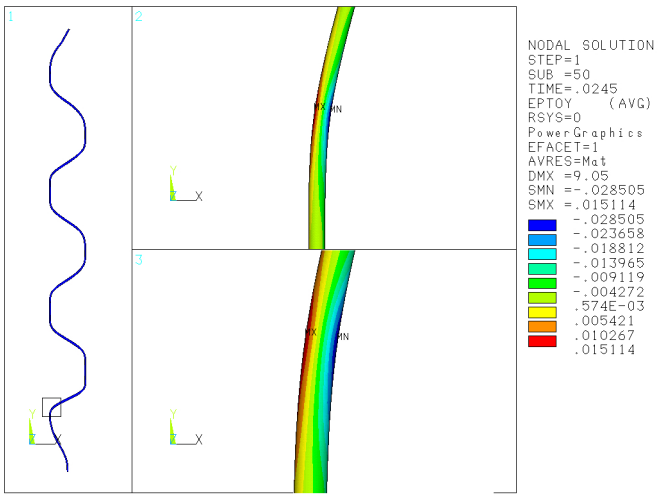

Figure 14. Peak cladding axial strain at t = 24.5 ms.

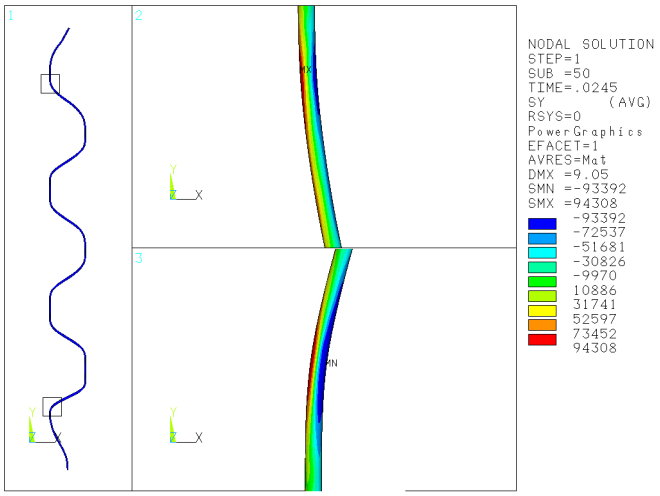

Figure 15. Peak cladding axial stress at t = 24.5 ms.

Limiting Case

The model used for the previous evaluation is based on the assumption that the fuel contributes only mass effects and no flexural rigidity to the pin buckling behavior. The primary reason for this assumption is that the fuel pellet/cladding interface is extremely complicated to characterize conservatively and very little information exists. If the strains in the previous evaluation were within acceptable limits regarding applicable failure modes, this model would have demonstrated convincingly that the integrity of the cladding material is preserved. However, the strains witnessed are in the range where potential failure of high- burn-up cladding materials cannot be clearly ruled out.

To assess the influence of the fuel's flexural rigidity on the buckling response, this case includes a full representation of the fuel pellets. The fuel pellets are assumed to be fully intact and fully adhered to the cladding and adjacent fuel pellets. The fuel is given elastic material properties for UO2 (specifically, E=12e6 psi, Poisson's ratio=0.3), and no internal pressurization is included.

Using the B&W 15x15 assembly configuration and the baseline conditions of the previous case, the results indicated that the pin would not buckle. The added rigidity prevented the initiation of buckling, and the pin exhibited a response characteristic of elastic stress wave propagation (Figure 16Figure 16Figure 16). The resulting strains (Figure 17Figure 17Figure 17) were essentially elastic due to axial loading and some bending of the initially curved fuel pin. As shown in Figure 17Figure 17Figure 17, the peak tensile and compressive strains only reach magnitudes of 0.00066 in/in and 0.00082 in/in (or 0.066% and 0.082%), respectively. This result is not unexpected, but it reemphasizes the influence the fuel pellets have on fuel pin axial impact response.

Conclusions

The resulting axial strains in the cladding ranged from 0.07- to 2.8% depending on the mechanical contribution of the fuel pellets. A conservative baseline case, which discounted the contribution of the fuel pellets to the pin's flexural rigidity and at the same time considered 100% of their mass contribution, yielded peak tensile and compressive strain magnitudes of 0.015 in/in and 0.028 in/in (or 1.5% and 2.8%), respectively. A limiting case,

involving full contribution of fuel pellets to flexural rigidity, yielded peak tensile and compressive strain magnitudes of 0.00066 in/in and 0.00082 in/in (or 0.066% and 0.082%), respectively.
Permissible strains regarding failure mechanisms for high- burn-up fuels are difficult to determine due to limited data, but ongoing work at PNNL has estimated that they are on the order of 1.7% to 3.0%. The analytical results from the baseline evaluation case are on the order of this estimated material limit. Clearly, results from this conservative baseline evaluation do not provide sufficient evidence that cladding failure cannot happen during end impacts typically experienced in a drop accident event (as defined by 10CFR71.73[3]). However, buckling did not occur and strains were very low when the fuel pellet flexural rigidity was fully accounted for and perfect bonding was assumed at the cladding-fuel pellet interface.
Since the strains yielded by the baseline evaluation model were nearly at an acceptable magnitude with the conservative assumption of neglecting fuel pellet flexural rigidity, a high degree of confidence regarding cladding survival is still expected. Results from assumptions inherent to the single pin model and additional conservatisms could be addressed further with a cask-fuel assembly model including 3D pin deformations, pin-pin interactions, spacer grid representation, etc.

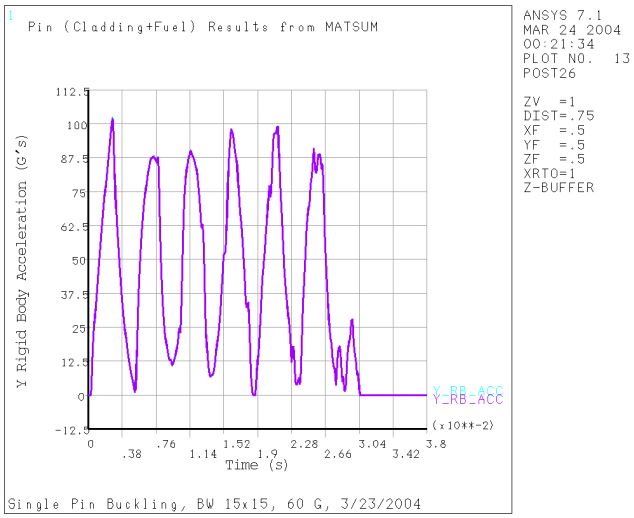

Figure 16. Pin rigid-body axial deceleration history.

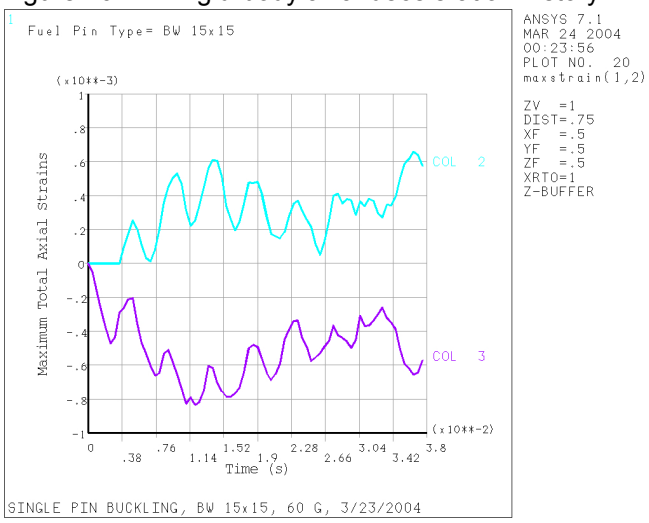

Figure 17. Cladding axial strain history.

Acknowledgments
The authors would like to thank Carl Beyer of Pacific Northwest National Laboratory for his contributions and assistance regarding high burn-up spent fuel material properties. The authors would also like to thank Gordon Bjorkman for his insightful comments and contributions on this study. Pacific Northwest National Laboratory is operated by Battelle under Contract DE-AC06-76RL01830.
References
[1] ANSYS®, Inc. 2003. “ANSYS®/LS-DYNA® User’s Guide.” in ANSYS Release 7.1 Documentation. Canonsburg, PA.

[2] Sanders TL, KD Seager, YR Rashid, PR Barrett, AP Malinauskas, RE Einziger, H Jordan, TA Duffey, SH Sutherland, and PC Reardon. 1992. A Method for Determining the Spent-Fuel Contribution to Transport Cask Containment Requirements. SAND90-2406, Sandia National Laboratories, Albuquerque, New Mexico.
[3] Title 10, Code of Federal Regulations, Part 71, Subpart 73, Packaging and Transportation of Radioactive Material,. Jan. 1, 2003, United States Government Printing Office, Washington, D.C.
[4] Bjorkman GS,. April 25-29, 2004,. "The Buckling of Fuel Rods in Transportation Casks Under Hypothetical Accident cConditions.", Proceedings ofrom the Twelfth International Conference on Nuclear Engineering, ICONE12-49554, Arlington VirginiaA.
[5] US Nuclear Regulatory Commission (USNRC). 1999. Buckling of Irradiated Fuel Under Bottom End Drop Conditions. ISG 12, Rev 1, Washington, DC.
[6] Electric Power Research Institute (EPRI). 1991. Fuel-Assembly Behavior Under Dynamic Impact Loads Due to Dry-Storage Cask Mishandling. EPRI-NP-7419, prepared by ABB Combustion Engineering, Inc. for Electric Power Research Institute, Palo Alto, CA.
[7] Roark RJ. , 1965. Formulas for Stress and Strain., 4th ed. McGraw-Hill, New York, NY.